Editors' Suggestion

Long-Distance Window of the Hadronic Vacuum Polarization for the Muon $g-2$

T. Blum,[1] P. A. Boyle,[2,3] M. Bruno,[4,5] B. Chakraborty,[6] F. Erben,[7] V. Gülpers,[3] A. Hackl,[8] N. Hermansson-Truedsson,[3] R. C. Hill,[3] T. Izubuchi,[2,9] L. Jin,[1] C. Jung,[2] C. Lehner,[8,*] J. McKeon,[6] A. S. Meyer,[10] M. Tomii,[1,9] J. T. Tsang,[7] and X.-Y. Tuo[2]

(RBC and UKQCD Collaborations)

[1]*Physics Department, University of Connecticut, Storrs, Connecticut 06269-3046, USA*
[2]*Physics Department, Brookhaven National Laboratory, Upton, New York 11973, USA*
[3]*School of Physics and Astronomy, The University of Edinburgh, Edinburgh EH9 3FD, United Kingdom*
[4]*Dipartimento di Fisica, Università di Milano-Bicocca, Piazza della Scienza 3, I-20126 Milano, Italy*
[5]*INFN, Sezione di Milano-Bicocca, Piazza della Scienza 3, I-20126 Milano, Italy*
[6]*School of Physics and Astronomy, University of Southampton, Southampton SO17 1BJ, United Kingdom*
[7]*CERN, Theoretical Physics Department, Geneva, Switzerland*
[8]*Fakultät für Physik, Universität Regensburg, Universitätsstraße 31, 93040 Regensburg, Germany*
[9]*RIKEN-BNL Research Center, Brookhaven National Laboratory, Upton, New York 11973, USA*
[10]*Nuclear and Chemical Sciences Division, Lawrence Livermore National Laboratory, Livermore, California 94550, USA*

(Received 31 October 2024; revised 26 March 2025; accepted 22 April 2025; published 19 May 2025)

We provide the first *ab initio* calculation of the Euclidean long-distance window of the isospin-symmetric light-quark connected contribution to the hadronic vacuum polarization for the muon $g-2$ and find $a_\mu^{\mathrm{LD,iso,conn,ud}} = 411.4(4.3)(2.4) \times 10^{-10}$. We also provide the currently most precise calculation of the total isospin-symmetric light-quark connected contribution, $a_\mu^{\mathrm{iso,conn,ud}} = 666.2(4.3)(2.5) \times 10^{-10}$ in the BMW20 world, which is more than 4σ larger compared to the data-driven estimates of Boito *et al.* [Phys. Rev. D **107**, 074001 (2023)] and 1.7σ larger compared to the lattice QCD result of BMW20.

DOI: 10.1103/PhysRevLett.134.201901

Introduction—The relative deviation of the muon's Landé factor g_μ from Dirac's relativistic quantum mechanics result, $a_\mu = (g_\mu - 2)/2$, also called the anomalous magnetic moment of the muon, is one of the most precisely determined quantities in particle physics. It is sensitive to virtual contributions of particles that may be out of reach of direct production in high-energy experiments, and it therefore plays an important role in constraining new physics. Substantial efforts have been undertaken at Fermilab (E989) and are planned at J-PARC (E34) [1] in order to further improve the precision of the experimental determination. In 2021 the Fermilab experiment released first results [2], which confirmed the previously best result obtained by the BNL E821 experiment [3] and reduced the experimental uncertainty from 0.54 ppm to 0.46 ppm. Subsequently they released results for runs II and III in 2023, which yielded an uncertainty of 0.2 ppm [4]. In 2025 the Fermilab experiment aims to release their final results pushing the uncertainty down to approximately 0.14 ppm [5].

Matching the precision of this spectacular experimental result in a theory calculation of the standard model (SM) contribution to a_μ is a substantial challenge and is currently a work in progress. In 2020 the Muon $g-2$ Theory Initiative published a white paper [6–26] that indicated a more than 4σ tension of the experimental result with the SM. This result relied on a data-driven estimate of the hadronic vacuum polarization (HVP) contribution based on $e^+e^- \to$ hadron experimental data. While existing tensions between experimental datasets had been taken into account in 2020 by inflating the uncertainties appropriately, the recent result by CMD-3 [27,28] increases the tensions to a degree that currently appears to make a data-driven high-precision evaluation of the HVP not feasible.

At the same time, lattice methodology is maturing and is on track to allow for a complete *ab initio* theory determination that soon may match the Fermilab E989 target precision. In this context, it is now common practice to separate the total HVP contribution into the Euclidean windows introduced in our previous work [29], which

*Contact author: christoph.lehner@ur.de

separate three different regions (short distance, intermediate distance, long distance) that exactly sum up to the total HVP. Each region has its own dominant challenges that can best be addressed by targeted calculations optimized separately for each region.

The short-distance region suffers from large discretization errors, and very fine lattices are needed. The intermediate-distance region has moderate uncertainties. The long-distance region suffers from large statistical and finite-size errors. For lattice calculations using rooted staggered quarks, additional challenges for the continuum limit of the long-distance contribution exist (see, e.g. Ref. [30]).

By now there is very good agreement among several lattice collaborations on the short-distance and intermediate-distance windows [30–42]. The same consolidation at high precision is also needed for the long-distance region, and the current Letter, which focuses on the dominant light-quark connected contribution, is a first step in this direction. The results reported in the following are unchanged compared to our unblinding presentation at Lattice 2024 [43].

In future work, we will improve our previous results [29] on the quark disconnected contributions and strong-isospin-breaking (SIB) and QED corrections, and improve our lattice spacing determinations to complete the calculation of a_μ at the next precision frontier. We note that a combination of lattice and data-driven methodology is also an interesting approach as suggested in Ref. [29] and recently demonstrated in Ref. [40].

Methodology—We address the particular challenges of the long-distance window by building on ideas of the improved bounding method [44] and finite-volume exclusive state reconstruction [45]. These methods express the leading-order HVP in terms of the time-momentum representation [46]

$$a_\mu = \sum_{t=0}^{\infty} w_t C(t) \tag{1}$$

with $C(t) = \frac{1}{3}\sum_{\vec{x}}\sum_{j=0,1,2}\langle J_j(\vec{x},t)J_j(0)\rangle$, vector current $J_\mu(x) = i\sum_f Q_f\bar{\Psi}_f(x)\gamma_\mu\Psi_f(x)$ with fractional electric charge Q_f, and sum over quark flavors f. The correlator $C(t)$ at zero temperature admits a spectral representation

$$C(t) = \frac{1}{3}\sum_{j=0,1,2}\sum_n |\langle n|\hat{J}_j|0\rangle|^2 e^{-E_n t} \tag{2}$$

with zero-momentum vector operator $\hat{J}_j$, Hamiltonian eigenstate $|n\rangle$, and energy E_n for the discrete finite-volume spectrum. The weights w_t can be discretized in different ways. We use the two approaches described in Ref. [31]. We separate the window contributions as in Ref. [29] into $a_\mu = a_\mu^{\rm SD} + a_\mu^{\rm W} + a_\mu^{\rm LD}$. We have $a_\mu^{\rm SD}(t_0,\Delta) = \sum_{t=0}^{\infty} C(t)w_t[1-\Theta(t,t_0,\Delta)]$, $a_\mu^{\rm W}(t_0,t_1,\Delta) = \sum_{t=0}^{\infty} C(t)w_t[\Theta(t,t_0,\Delta)-\Theta(t,t_1,\Delta)]$, and $a_\mu^{\rm LD}(t_1,\Delta) = \sum_{t=0}^{\infty} C(t)w_t\Theta(t,t_1,\Delta)$ with $\Theta(t,t',\Delta) = \{1+\tanh[(t-t')/\Delta]\}/2$. We select $t_0 = 0.4$ fm, $t_1 = 1.0$ fm, and $\Delta = 0.15$ fm as suggested in Ref. [29].

TABLE I. List of $N_f = 2+1$ ensembles with parameters determined in the RBC/UKQCD18 isospin-symmetric world defined in Eq. (3). The ensembles have Iwasaki gauge action and Möbius [53] domain-wall [54,55] fermion sea quarks with $b = 1.5$ and $c = 0.5$. The parameters b and c are defined in Ref. [56]. The masses include finite-volume corrections and are obtained from a combined fit of all ensembles that only differ by the lattice volume. The scripts generating the new ensembles are publicly available [52].

ID	a^{-1}/GeV	$L^3\times T\times L_s/a^5$	m_π/MeV	m_K/MeV	$m_\pi L$
96I	2.6920(67)	$96^3\times 192\times 12$	131.29(66)	484.5(2.3)	4.7
64I	2.3549(49)	$64^3\times 128\times 12$	138.98(43)	507.5(1.5)	3.8
48I	1.7312(28)	$48^3\times 96\times 24$	139.32(30)	499.44(88)	3.9
C	1.7312(28)	$64^3\times 96\times 24$	139.32(30)	499.44(88)	5.2
4	1.7312(28)	$24^3\times 48\times 24$	274.8(2.5)	530.1(3.1)	3.8
D	1.7312(28)	$32^3\times 48\times 24$	274.8(2.5)	530.1(3.1)	5.1
1	1.7312(28)	$32^3\times 64\times 24$	208.1(1.1)	514.0(1.8)	3.8
3	1.7312(28)	$32^3\times 64\times 24$	211.3(2.3)	603.8(6.1)	3.9
9	2.3549(49)	$32^3\times 64\times 12$	278.9(0.6)	531.2(0.7)	3.8
L	2.3549(49)	$64^3\times 128\times 12$	278.9(0.6)	531.2(0.7)	7.6

The correlators $C(t)$ are computed with a hierarchical approximation scheme [29,47,48] using locally coherent low modes with exact eigenvalues [49]. In addition, as described in Ref. [44], we use exact distillation [50,51] and have made our code publicly available [52].

In Table I we provide a list of all lattice gauge ensembles used in this study. For the physical pion mass ensembles with $m_\pi L \approx 5$ (96I and C) we use 200 Laplace eigenmodes and for all other ensembles we use 60. We use an operator basis including a local vector current, a distillation-smeared vector current, and two-pion operators up to a relative momentum of $p = (2,0,0)(2\pi/L)$ for the case of 60 Laplace eigenmodes and $p = (2,2,0)(2\pi/L)$ for the case of 200 Laplace eigenmodes. All operators are in the T_1^u, $I = 1$ irreducible representation since we focus on the dominant light-quark connected contribution.

In Fig. 1, we demonstrate the reconstruction of the first N states via $C^N(t) = (1/3)\sum_{j=0,1,2}\sum_{n=1}^{N}|\langle n|\hat{J}_j|0\rangle|^2 e^{-E_n t}$ compared to the full $C(t)$. The figure shows the result of using only distillation-smeared operators (vector and two-pion) in a generalized eigenvalue problem study [57,58] to find the E_n and optimal operators to project to a given state $|n\rangle$. This operator is contracted with the local vector current to obtain the overlap factor $|\langle n|\hat{J}_j|0\rangle|^2$. The reconstruction $C^N(t)$ is used at large Euclidean times t, where $C^N(t) = C(t)$ within statistical uncertainties.

As in our previous work [31], we perform the analysis in a blinded manner with five analysis groups A–E.

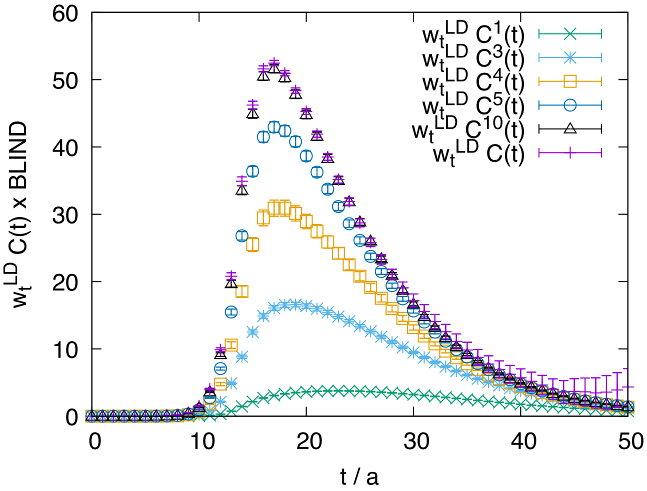

FIG. 1. Reconstruction of the lowest N states $C^N(t)$ compared to the inclusive $C(t)$ for the 96I ensemble with $w_t^{\rm LD} = w_t\Theta(t, t_1, \Delta)$. The exponential growth of statistical noise in $C(t)$ is absent in the reconstruction.

Four analysis groups A–D have conducted a full analysis, while one group (E) has focused on cross-checks. Each analysis group received the correlator data with a blinding factor applied to each insertion of a local vector current. The blinding factor was unique to each group and generated using a hash function based on the group's name (A–E). The blinding factors were applied by a script, and no one in the collaboration saw the blinding factors themselves. The process was managed by one of the authors (C. L.). Once the analysis groups were ready, relative unblinding meetings between two analysis groups were organized in which the respective methods were scrutinized. After conclusion of this process the relative blinding factor was removed between the participating groups. After the relative unblinding, the collaboration agreed to the RBC/UKQCD24 prescription for the analysis that will be described in detail in the following. This procedure was then applied to a final analysis before the absolute blinding was removed in a joint meeting on July 19, 2024. The absolute blinding factor is still applied to the figures of this Letter apart from Fig. 5. It can be removed by dividing by the blinding factor (BLIND) of 1.9296.

The cross-checks of group E were conducted prior to the unblinding and focused on results that were not affected by the blinding factor such as the ratio of $C^N(t)$ to $C(t)$ for which the blinding factor drops out, as well as checks of individual E_n that are also not affected by the blinding. Additional details on the cross-checks and on the various methods studied by the individual groups are provided as Supplemental Material [59] to this Letter.

The calculation of $C(t)$ is organized as an expansion around an isospin-symmetric point [29,60–64]. In this Letter, we provide results for two choices of the expansion point, following our earlier work [31]. The first choice is the RBC/UKQCD18 world defined by

$$m_\pi = 0.135\ \text{GeV}, \qquad m_K = 0.4957\ \text{GeV}, \qquad m_\Omega = 1.67225\ \text{GeV}, \tag{3}$$

consistent with Ref. [29]. We also consider a second choice

$$m_\pi = 0.13497\ \text{GeV}, \qquad m_{ss*} = 0.6898\ \text{GeV}, \qquad w_0 = 0.17236\ \text{fm}, \tag{4}$$

which we label as the BMW20 world [30]. We define m_{ss*} as the ground-state energy of the quark-connected pseudoscalar $\bar{s}s$ meson two-point function. To avoid an unnecessary inflation of uncertainties when comparing isospin-symmetric lattice results, we define the above values without uncertainties. The experimental uncertainties of the physical hadron spectrum enter when quantum electrodynamics (QED) and SIB corrections are included.

Finite-volume corrections are applied using the Hansen-Patella formalism [65,66] in the monopole approximation. As can be seen in Fig. 2, after applying finite-volume corrections the results for ensembles that only differ by the lattice volume (4 and D, 9 and L, 48I and C) agree within uncertainties. We provide a detailed study of the agreement as a function of Euclidean time in Supplemental Material [59]. It is noteworthy that for our largest volume with $m_\pi L = 7.6$(L), the finite-volume corrections are smaller than the quoted statistical uncertainties.

Analysis and results—In the following, we describe the RBC/UKQCD24 prescription for determining the light-quark connected contribution to the long-distance window in the isospin-symmetric limit, $a_\mu^{\rm LD,iso,conn,ud}$.

For each ensemble in Table I, the long-distance part of $C(t)$ is replaced by $C^N(t)$ for sufficiently large times such that they agree within statistical uncertainties. For the ensembles with 200 Laplace modes $N = 10$ and for all other ensembles $N = 5$. In all cases this allows for a spectral reconstruction beyond the peak of the rho resonance. Finite-volume corrections are applied as shown in Fig. 2. These data points are fit jointly to several fit functions. We study both an additive and a multiplicative combination of discretization and mass-mistuning effects by varying between

$$\begin{aligned} f_+ = f_0 + f_1 a^2 &+ f_2[w_0 m_\pi - (w_0 m_\pi)_{\rm phys}] \\ &+ f_3[w_0 m_\pi - (w_0 m_\pi)_{\rm phys}]^2 \\ &+ f_4[w_0 m_{ss*} - (w_0 m_{ss*})_{\rm phys}] \end{aligned} \tag{5}$$

and

$$\begin{aligned} f_* = f_0(1 + f_1 a^2)\{1 &+ f_2[w_0 m_\pi - (w_0 m_\pi)_{\rm phys}] \\ &+ f_3[w_0 m_\pi - (w_0 m_\pi)_{\rm phys}]^2 \\ &+ f_4[w_0 m_{ss*} - (w_0 m_{ss*})_{\rm phys}]\}. \end{aligned} \tag{6}$$

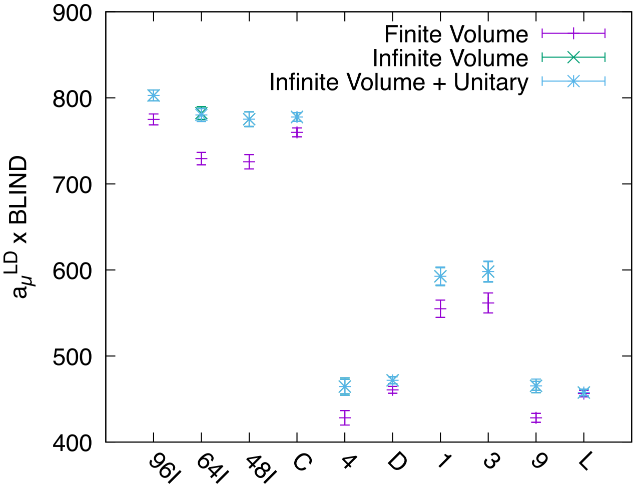

FIG. 2. Results for the ensembles listed in Table I with and without finite-volume corrections applied. For ensemble 64I a small correction from the partially quenched point to the unitary point is added as well (see Ref. [31]).

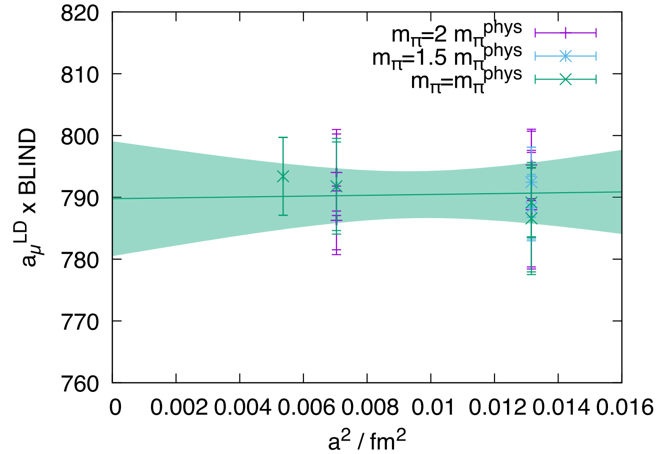

FIG. 3. Fit result of f_* with Z_V^π and without setting $f_3 = 0$. The data are shown for all ensembles as a function of a^2 after subtracting the fit function without the $f_0 f_1 a^2$ term.

The functional forms as given apply to the BMW20 world, and the dimensionless ratios $w_0 m_\pi$ and $w_0 m_{ss*}$ have to be replaced with m_π/m_Ω and m_K/m_Ω for the RBC/UKQCD18 world. For both fit functions, we also study versions with $f_3 = 0$. These four fit forms are then applied to the data renormalized with two different choices for the local vector current renormalization constant: Z_V^π and $Z_V^\star$. The former is defined by the pion charge, the latter by the ratio of local-conserved to local-local correlators at a distance of 1 fm. This results in 8 fits that are then combined in a model average. All fit forms have acceptable p-value and the results are consistent between using the Akaike information criterion [67], a simple χ^2 weight, and a flat weight of all models. We provide individual results in Supplemental Material [59]. We also studied more divergent chiral dependencies; however, since our analysis is dominated by four ensembles at physical pion mass, such variations have little impact on the fit results. In Fig. 3, we show the fit result of f_* with Z_V^π and without setting $f_3 = 0$. We emphasize that the extrapolation to the continuum limit is within the statistical uncertainties of the finest data point.

In Fig. 4, we compare the results obtained by the different analysis groups to the RBC/UKQCD24 prescription. We observed good agreement prior to the absolute unblinding and have identified the reasons for the residual variations. We note that group D only took the continuum limit of physical pion mass ensembles. Groups A and B also verified the consistency of the continuum limits with and without ensembles 9 and L. The lattice spacing uncertainty due to our more limited knowledge of the Ω^- mass is responsible for the larger errors in RBC/UKQCD18 world. Work on a more precise determination of m_Ω is in progress. We observe that RBC/UKQCD18 and BMW20 worlds are consistent at the current precision.

Our final results are

$$a_\mu^{\text{LD,iso,conn,ud}} = 411.4(4.3)(2.4) \times 10^{-10},$$
$$a_\mu^{\text{iso,conn,ud}} = 666.2(4.3)(2.5) \times 10^{-10} \qquad (7)$$

in the BMW20 world and

$$a_\mu^{\text{LD,iso,conn,ud}} = 413.6(6.0)(2.9) \times 10^{-10},$$
$$a_\mu^{\text{iso,conn,ud}} = 668.7(6.1)(2.9) \times 10^{-10} \qquad (8)$$

in the RBC/UKQCD18 world, where the first error is statistical and the second systematic. We provide additional details for the systematic uncertainties in Supplemental Material [59]. The total isospin-symmetric results are obtained by adding our previous short-distance and intermediate-distance results [31].

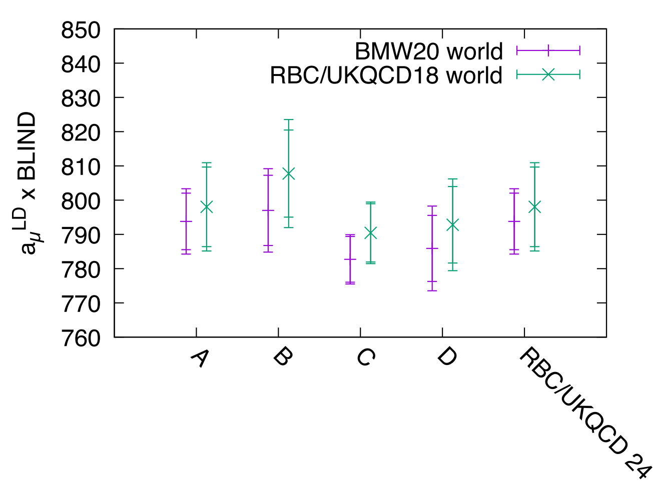

FIG. 4. Results obtained by the different analysis groups and the resulting RBC/UKQCD24 prescription.

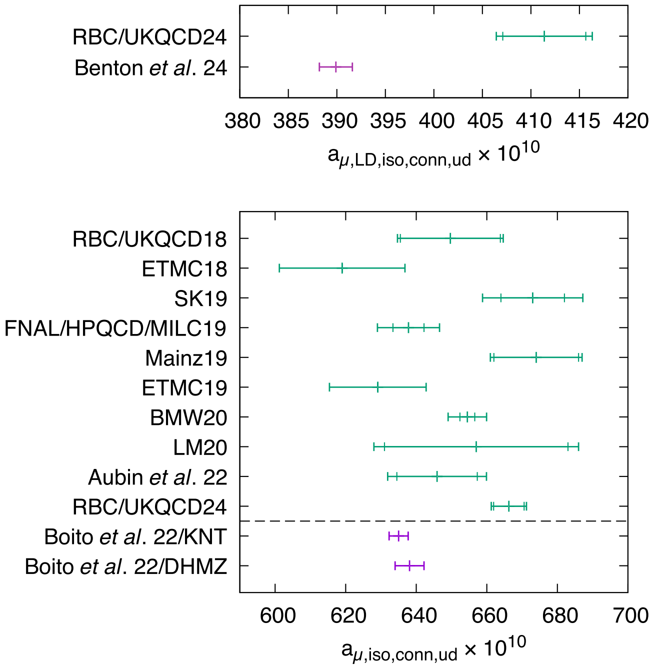

FIG. 5. This work compared to the literature: Benton *et al.* 24 [70], RBC/UKQCD18 [29], ETMC18 [71], SK19 [72], FNAL/HPQCD/MILC19 [73], Mainz19 [74], ETMC19 [75], BMW20 [30], LM20 [34], Aubin *et al.* 22 [35], and Boito *et al.* 22/KNT and Boito *et al.* 22/DHMZ [69].

In Fig. 5, we compare our results in the BMW20 world to the literature [68]. Our result for $a_\mu^{\mathrm{iso,conn,ud}}$ is more than 4σ larger compared to the data-driven estimates by Boito *et al.* [69], which were obtained based on the datasets that entered the Theory Initiative white paper [6] prior to the release of the CMD-3 data. This observed shift with respect to the data-driven estimate is consistent with the size of the tension between experiment and theory for the muon $g-2$ quoted in the 2020 white paper of the Muon $g-2$ Theory Initiative [6]. Finally, we note that our result is also 1.7σ larger compared to the lattice QCD result of BMW20 [30].

Conclusions and outlook—In this Letter we compute the long-distance Euclidean window of the hadronic vacuum polarization for light quarks in the isospin-symmetric limit. This calculation is particularly challenging and dominates the total uncertainty of a complete high-precision $a_\mu^{\mathrm{HVP\,LO}}$ result obtained from first-principles lattice QCD methods. All calculations were performed in a blinded manner. We find a large tension with the data-driven approach [69] based on datasets that were also used in Ref. [6] but also a smaller tension with the BMW20 result [30]. More work is needed to complete an *ab initio* calculation matching the Fermilab E989 target precision. We are currently improving our previous estimates for the quark-disconnected contributions and the QED and SIB corrections including diagrams beyond the electroquenched approximation. We expect to match the FNAL E989 target precision upon completion of our HVP program.

Acknowledgments—We thank our colleagues of the RBC and UKQCD collaborations for many valuable discussions and joint efforts over the years. The authors gratefully acknowledge the Gauss Centre for Supercomputing e.V. [76] for funding this project by providing computing time on the GCS Supercomputer JUWELS at Jülich Supercomputing Centre (JSC). We acknowledge the EuroHPC Joint Undertaking for awarding this project access to the EuroHPC supercomputer LUMI, hosted by CSC (Finland) and the LUMI consortium through a EuroHPC Extreme Scale Access call as well as the EuroHPC supercomputer LEONARDO, hosted by CINECA (Italy). An award of computer time was provided by the ASCR Leadership Computing Challenge (ALCC) and Innovative and Novel Computational Impact on Theory and Experiment (INCITE) programs. This research used resources of the Argonne Leadership Computing Facility, which is a DOE Office of Science User Facility supported under Contract No. DE-AC02-06CH11357. This research also used resources of the Oak Ridge Leadership Computing Facility, which is a DOE Office of Science User Facility supported under Contract No. DE-AC05-00OR22725. This research used resources of the National Energy Research Scientific Computing Center (NERSC), a U.S. Department of Energy Office of Science User Facility located at Lawrence Berkeley National Laboratory, operated under Contract No. DE-AC02-05CH11231 using NERSC Award No. NESAP m1759 for 2020. This work used the DiRAC Blue Gene Q Shared Petaflop system at the University of Edinburgh, operated by the Edinburgh Parallel Computing Centre on behalf of the STFC DiRAC HPC Facility [77]. This equipment was funded by BIS National E-infrastructure capital Grant No. ST/K000411/1, STFC capital Grant No. ST/H008845/1, and STFC DiRAC Operations Grants No. ST/K005804/1 and No. ST/K005790/1. DiRAC is part of the National E-Infrastructure. We gratefully acknowledge disk and tape storage provided by USQCD and by the University of Regensburg with support from the DFG. The lattice data analyzed in this project was generated using GPT [52], Grid [78–80], and CPS [81,82] and analyzed, in part, using pyobs [83]. T. B. is supported by the U.S. DOE under Grant No. DE-SC0010339. P. B., T. I., and C. J. were supported in part by U.S. DOE Contract No. DESC0012704(BNL) and the Scientific Discovery through Advanced Computing (SciDAC) program LAB 22-2580. At the beginning of the project, M. B. was supported by the national program for young researchers "Rita Levi Montalcini." M. B. is (partially) supported by ICSC-Centro Nazionale di Ricerca in High Performance Computing, Big Data and Quantum Computing, funded by European Union—NextGenerationEU. Research of B. C. at the University of Southampton has been supported by the following research fellowship and grants: Leverhulme Trust (ECF-2019-223 G100820), STFC

(Grant No. ST/X000583/1), STFC (Grant No. ST/W006251/1), and EPSRC (Grant No. EP/W032635/1). F. E. has received funding from the European Union's Horizon Europe research and innovation programme under the Marie Skłodowska-Curie Grant No. 101106913. V. G. is supported in part by UK STFC Grants No. ST/P000630/1, No. ST/T000600/1, and No. ST/X000494/1. A. H. is supported by the Hans-Böckler-Stiftung. N. H. T. is funded by the UK Research and Innovation, Engineering and Physical Sciences Research Council, Grant No. EP/X021971/1. R. H. is supported by UK STFC Grant No. ST/P000630/1. T. I. is also supported by the Department of Energy, Laboratory Directed Research and Development (LDRD No. 23-051) of BNL and RIKEN BNL Research Center. L. J. and M. T. acknowledge the support of DOE Office of Science Early Career Award No. DE-SC0021147 and DOE Grant No. DE-SC0010339. A. S. M. is supported in part by Lawrence Livermore National Security, LLC No. DE-AC52-07NA27344, Neutrino Theory Network Program Grant No. DE-AC02-07CHI11359, and the U.S. Department of Energy Award No. DE-SC0020250. X. Y. T. has been supported by U.S. DOE Contract No. DESC0012704(BNL).

[1] M. Abe *et al.*, A new approach for measuring the muon anomalous magnetic moment and electric dipole moment, Prog. Theor. Exp. Phys. **2019**, 053C02 (2019).

[2] B. Abi *et al.* (Muon g-2 Collaboration), Measurement of the positive muon anomalous magnetic moment to 0.46 ppm, Phys. Rev. Lett. **126**, 141801 (2021).

[3] G. Bennett *et al.* (Muon g-2 Collaboration), Final report of the muon E821 anomalous magnetic moment measurement at BNL, Phys. Rev. D **73**, 072003 (2006).

[4] D. P. Aguillard *et al.* (Muon g-2 Collaboration), Measurement of the positive muon anomalous magnetic moment to 0.20 ppm, Phys. Rev. Lett. **131**, 161802 (2023).

[5] R. Carey, K. Lynch, J. Miller, B. Roberts, W. Morse *et al.*, The new (g-2) experiment: A proposal to measure the muon anomalous magnetic moment to ±0.14 ppm precision (2009), 10.2172/952029.

[6] T. Aoyama *et al.*, The anomalous magnetic moment of the muon in the standard model, Phys. Rep. **887**, 1 (2020).

[7] T. Aoyama, M. Hayakawa, T. Kinoshita, and M. Nio, Complete tenth-order QED contribution to the muon $g-2$, Phys. Rev. Lett. **109**, 111808 (2012).

[8] T. Aoyama, T. Kinoshita, and M. Nio, Theory of the anomalous magnetic moment of the electron, Atoms **7**, 28 (2019).

[9] A. Czarnecki, W. J. Marciano, and A. Vainshtein, Refinements in electroweak contributions to the muon anomalous magnetic moment, Phys. Rev. D **67**, 073006 (2003); **73**, 119901(E) (2006).

[10] C. Gnendiger, D. Stöckinger, and H. Stöckinger-Kim, The electroweak contributions to $(g-2)_\mu$ after the Higgs boson mass measurement, Phys. Rev. D **88**, 053005 (2013).

[11] M. Davier, A. Hoecker, B. Malaescu, and Z. Zhang, Reevaluation of the hadronic vacuum polarisation contributions to the standard model predictions of the muon $g-2$ and $\alpha(m_Z^2)$ using newest hadronic cross-section data, Eur. Phys. J. C **77**, 827 (2017).

[12] A. Keshavarzi, D. Nomura, and T. Teubner, Muon $g-2$ and $\alpha(M_Z^2)$: A new data-based analysis, Phys. Rev. D **97**, 114025 (2018).

[13] G. Colangelo, M. Hoferichter, and P. Stoffer, Two-pion contribution to hadronic vacuum polarization, J. High Energy Phys. 02 (2019) 006.

[14] M. Hoferichter, B.-L. Hoid, and B. Kubis, Three-pion contribution to hadronic vacuum polarization, J. High Energy Phys. 08 (2019) 137.

[15] M. Davier, A. Hoecker, B. Malaescu, and Z. Zhang, A new evaluation of the hadronic vacuum polarisation contributions to the muon anomalous magnetic moment and to $\boldsymbol{\alpha(m_Z^2)}$, Eur. Phys. J. C **80**, 241 (2020); **80**, 410(E) (2020).

[16] A. Keshavarzi, D. Nomura, and T. Teubner, The $g-2$ of charged leptons, $\alpha(M_Z^2)$ and the hyperfine splitting of muonium, Phys. Rev. D **101**, 014029 (2020).

[17] A. Kurz, T. Liu, P. Marquard, and M. Steinhauser, Hadronic contribution to the muon anomalous magnetic moment to next-to-next-to-leading order, Phys. Lett. B **734**, 144 (2014).

[18] K. Melnikov and A. Vainshtein, Hadronic light-by-light scattering contribution to the muon anomalous magnetic moment revisited, Phys. Rev. D **70**, 113006 (2004).

[19] P. Masjuan and P. Sánchez-Puertas, Pseudoscalar-pole contribution to the $(g_\mu-2)$: A rational approach, Phys. Rev. D **95**, 054026 (2017).

[20] G. Colangelo, M. Hoferichter, M. Procura, and P. Stoffer, Dispersion relation for hadronic light-by-light scattering: Two-pion contributions, J. High Energy Phys. 04 (2017) 161.

[21] M. Hoferichter, B.-L. Hoid, B. Kubis, S. Leupold, and S. P. Schneider, Dispersion relation for hadronic light-by-light scattering: Pion pole, J. High Energy Phys. 10 (2018) 141.

[22] A. Gérardin, H. B. Meyer, and A. Nyffeler, Lattice calculation of the pion transition form factor with $N_f=2+1$ Wilson quarks, Phys. Rev. D **100**, 034520 (2019).

[23] J. Bijnens, N. Hermansson-Truedsson, and A. Rodríguez-Sánchez, Short-distance constraints for the HLbL contribution to the muon anomalous magnetic moment, Phys. Lett. B **798**, 134994 (2019).

[24] G. Colangelo, F. Hagelstein, M. Hoferichter, L. Laub, and P. Stoffer, Longitudinal short-distance constraints for the hadronic light-by-light contribution to $(g-2)_\mu$ with large-N_c Regge models, J. High Energy Phys. 03 (2020) 101.

[25] T. Blum, N. Christ, M. Hayakawa, T. Izubuchi, L. Jin, C. Jung, and C. Lehner, The hadronic light-by-light scattering contribution to the muon anomalous magnetic moment from lattice QCD, Phys. Rev. Lett. **124**, 132002 (2020).

[26] G. Colangelo, M. Hoferichter, A. Nyffeler, M. Passera, and P. Stoffer, Remarks on higher-order hadronic corrections to the muon $g-2$, Phys. Lett. B **735**, 90 (2014).

[27] F. V. Ignatov *et al.* (CMD-3 Collaboration), Measurement of the pion form factor with CMD-3 detector and its implication to the hadronic contribution to muon (g-2), Phys. Rev. Lett. **132**, 231903 (2024).

[28] F. V. Ignatov *et al.* (CMD-3 Collaboration), Measurement of the $e+e- \to \pi+\pi-$ cross section from threshold to 1.2 GeV with the CMD-3 detector, Phys. Rev. D **109**, 112002 (2024).

[29] T. Blum, P. A. Boyle, V. Gülpers, T. Izubuchi, L. Jin, C. Jung, A. Jüttner, C. Lehner, A. Portelli, and J. T. Tsang (RBC, UKQCD Collaborations), Calculation of the hadronic vacuum polarization contribution to the muon anomalous magnetic moment, Phys. Rev. Lett. **121**, 022003 (2018).

[30] S. Borsanyi *et al.*, Leading hadronic contribution to the muon magnetic moment from lattice QCD, Nature (London) **593**, 51 (2021).

[31] T. Blum *et al.* (RBC, UKQCD Collaborations), Update of euclidean windows of the hadronic vacuum polarization, Phys. Rev. D **108**, 054507 (2023).

[32] C. Aubin, T. Blum, C. Tu, M. Golterman, C. Jung, and S. Peris, Light quark vacuum polarization at the physical point and contribution to the muon $g-2$, Phys. Rev. D **101**, 014503 (2020).

[33] D. Giusti and S. Simula, Window contributions to the muon hadronic vacuum polarization with twisted-mass fermions, Proc. Sci. LATTICE2021 (**2022**) 189 [arXiv:2111.15329].

[34] C. Lehner and A. S. Meyer, Consistency of hadronic vacuum polarization between lattice QCD and the r-ratio, Phys. Rev. D **101**, 074515 (2020).

[35] C. Aubin, T. Blum, M. Golterman, and S. Peris, Muon anomalous magnetic moment with staggered fermions: Is the lattice spacing small enough?, Phys. Rev. D **106**, 054503 (2022).

[36] G. Wang, T. Draper, K.-F. Liu, and Y.-B. Yang (chiQCD Collaboration), Muon g-2 with overlap valence fermion, Phys. Rev. D **107**, 034513 (2023).

[37] M. Cè *et al.*, Window observable for the hadronic vacuum polarization contribution to the muon $g-2$ from lattice QCD, Phys. Rev. D **106**, 114502 (2022).

[38] C. Alexandrou *et al.*, Lattice calculation of the short and intermediate time-distance hadronic vacuum polarization contributions to the muon magnetic moment using twisted-mass fermions, Phys. Rev. D **107**, 074506 (2023).

[39] A. Bazavov *et al.*, Light-quark connected intermediate-window contributions to the muon $g-2$ hadronic vacuum polarization from lattice QCD, Phys. Rev. D **107**, 114514 (2023).

[40] A. Boccaletti *et al.*, High precision calculation of the hadronic vacuum polarisation contribution to the muon anomaly, arXiv:2407.10913.

[41] S. Kuberski, M. Cè, G. von Hippel, H. B. Meyer, K. Ottnad, A. Risch, and H. Wittig, Hadronic vacuum polarization in the muon g − 2: The short-distance contribution from lattice QCD, J. High Energy Phys. 03 (2024) 172.

[42] S. Spiegel and C. Lehner, A high-precision continuum limit study of the HVP short-distance window, arXiv:2410.17053.

[43] C. Lehner *et al.*, Status of the RBC/UKQCD HVP program, *Proceedings of the 41st International Symposium on Lattice Field Theory* (2024), https://conference.ippp.dur.ac.uk/event/1265/contributions/7454/attachments/5725/7497/talk.pdf.

[44] M. Bruno, T. Izubuchi, C. Lehner, and A. S. Meyer, Exclusive channel study of the muon HVP, Proc. Sci. LATTICE2019 (**2019**) 239 [arXiv:1910.11745].

[45] M. Della Morte *et al.*, A lattice calculation of the hadronic vacuum polarization contribution to $(g-2)_\mu$, EPJ Web Conf. **175**, 06031 (2018).

[46] D. Bernecker and H. B. Meyer, Vector correlators in lattice QCD: Methods and applications, Eur. Phys. J. A **47**, 148 (2011).

[47] T. Blum, T. Izubuchi, and E. Shintani, New class of variance-reduction techniques using lattice symmetries, Phys. Rev. D **88**, 094503 (2013).

[48] E. Shintani, R. Arthur, T. Blum, T. Izubuchi, C. Jung, and C. Lehner, Covariant approximation averaging, Phys. Rev. D **91**, 114511 (2015).

[49] M. A. Clark, C. Jung, and C. Lehner, *Multi-grid Lanczos, in 35th International Symposium on Lattice Field Theory (Lattice 2017) Granada, Spain, 2017* (2017), arXiv:1710.06884.

[50] M. Peardon, J. Bulava, J. Foley, C. Morningstar, J. Dudek, R. G. Edwards, B. Joo, H.-W. Lin, D. G. Richards, and K. J. Juge (Hadron Spectrum Collaboration), A novel quark-field creation operator construction for hadronic physics in lattice QCD, Phys. Rev. D **80**, 054506 (2009).

[51] M. Bruno, D. Hoying, T. Izubuchi, C. Lehner, A. S. Meyer, and M. Tomii, Isospin 0 and 2 two-pion scattering at physical pion mass using distillation with periodic boundary conditions in lattice QCD, arXiv:2304.03313.

[52] C. Lehner *et al.*, Grid Python Toolkit (GPT), https://github.com/lehner/gpt.

[53] R. C. Brower, H. Neff, and K. Orginos, The Möbius domain wall fermion algorithm, Comput. Phys. Commun. **220**, 1 (2017).

[54] Y. Shamir, Chiral fermions from lattice boundaries, Nucl. Phys. **B406**, 90 (1993).

[55] V. Furman and Y. Shamir, Axial symmetries in lattice QCD with Kaplan fermions, Nucl. Phys. **B439**, 54 (1995).

[56] T. Blum *et al.* (RBC, UKQCD Collaborations), Domain wall QCD with physical quark masses, Phys. Rev. D **93**, 074505 (2016).

[57] M. Luscher and U. Wolff, How to calculate the elastic scattering matrix in two-dimensional quantum field theories by numerical simulation, Nucl. Phys. **B339**, 222 (1990).

[58] B. Blossier, M. Della Morte, G. von Hippel, T. Mendes, and R. Sommer, On the generalized eigenvalue method for energies and matrix elements in lattice field theory, J. High Energy Phys. 04 (2009) 094.

[59] See Supplemental Material at http://link.aps.org/supplemental/10.1103/PhysRevLett.134.201901 for further details on the uncertainty estimates provided in this letter.

[60] G. M. de Divitiis, R. Frezzotti, V. Lubicz, G. Martinelli, R. Petronzio, G. C. Rossi, F. Sanfilippo, S. Simula, and N. Tantalo (RM123 Collaboration), Leading isospin breaking effects on the lattice, Phys. Rev. D **87**, 114505 (2013).

[61] P. Boyle, V. Gülpers, J. Harrison, A. Jüttner, C. Lehner, A. Portelli, and C. T. Sachrajda, Isospin breaking corrections to meson masses and the hadronic vacuum polarization: A comparative study, J. High Energy Phys. 09 (2017) 153.

[62] D. Giusti, V. Lubicz, G. Martinelli, F. Sanfilippo, and S. Simula, Electromagnetic and strong isospin-breaking corrections to the muon $g-2$ from lattice QCD + QED, Phys. Rev. D **99**, 114502 (2019).

[63] M. Di Carlo, G. Martinelli, D. Giusti, V. Lubicz, C. T. Sachrajda, F. Sanfilippo, S. Simula, and N. Tantalo, Light-meson leptonic decay rates in lattice QCD + QED, Phys. Rev. D **100**, 034514 (2019).

[64] P. Boyle *et al.*, Isospin-breaking corrections to light-meson leptonic decays from lattice simulations at physical quark masses, J. High Energy Phys. 02 (2023) 242.
[65] M. T. Hansen and A. Patella, Finite-volume effects in $(g-2)_\mu^{\mathrm{HVP,LO}}$, Phys. Rev. Lett. **123**, 172001 (2019).
[66] M. T. Hansen and A. Patella, Finite-volume and thermal effects in the leading-HVP contribution to muonic $(g-2)$, J. High Energy Phys. 10 (2020) 029.
[67] H. Akaike, A new look at the statistical model identification, IEEE Trans. Autom. Control **19**, 716 (1974).
[68] We note that after the unblinding of our result at Lattice 2024 in July of 2024, at the KEK workshop of the Muon g-2 Theory Initiative in September of 2024 unblinded results for $a_\mu^{\mathrm{LD,iso,conn,ud}}$ and $a_\mu^{\mathrm{iso,conn,ud}}$ were presented by the Mainz Collaboration. At the point of finalizing this manuscript the Mainz result had not yet appeared in the literature.
[69] D. Boito, M. Golterman, K. Maltman, and S. Peris, Data-based determination of the isospin-limit light-quark-connected contribution to the anomalous magnetic moment of the muon, Phys. Rev. D **107**, 074001 (2023).
[70] G. Benton, D. Boito, M. Golterman, A. Keshavarzi, K. Maltman, and S. Peris, Data-driven results for light-quark connected and strange-plus-disconnected hadronic $g-2$ short- and long-distance windows, Phys. Rev. D **111**, 034018 (2025).
[71] D. Giusti, F. Sanfilippo, and S. Simula, Light-quark contribution to the leading hadronic vacuum polarization term of the muon $g-2$ from twisted-mass fermions, Phys. Rev. D **98**, 114504 (2018).
[72] E. Shintani and Y. Kuramashi (PACS Collaboration), Hadronic vacuum polarization contribution to the muon $g-2$ with $2+1$ flavor lattice QCD on a larger than $(10\ \mathrm{fm})^4$ lattice at the physical point, Phys. Rev. D **100**, 034517 (2019).
[73] C. T. H. Davies *et al.* (Fermilab Lattice, LATTICE-HPQCD, MILC Collaborations), Hadronic-vacuum-polarization contribution to the muon's anomalous magnetic moment from four-flavor lattice QCD, Phys. Rev. D **101**, 034512 (2020).
[74] A. Gérardin, M. Cè, G. von Hippel, B. Hörz, H. B. Meyer, D. Mohler, K. Ottnad, J. Wilhelm, and H. Wittig, The leading hadronic contribution to $(g-2)_\mu$ from lattice QCD with $N_\mathrm{f}=2+1$ flavours of $\mathrm{O}(a)$ improved Wilson quarks, Phys. Rev. D **100**, 014510 (2019).
[75] D. Giusti and S. Simula, Lepton anomalous magnetic moments in lattice QCD + QED, Proc. Sci. LATTICE2019 (**2019**) 104 [arXiv:1910.03874].
[76] www.gauss-centre.eu
[77] www.dirac.ac.uk
[78] P. A. Boyle *et al.*, Grid, https://github.com/paboyle/Grid.
[79] P. A. Boyle, G. Cossu, A. Yamaguchi, and A. Portelli, Grid: A next generation data parallel C++ QCD library, Proc. Sci. LATTICE2015 (**2016**) 023.
[80] A. Yamaguchi, P. Boyle, G. Cossu, G. Filaci, C. Lehner, and A. Portelli, Grid: OneCode and FourAPIs, Proc. Sci. LATTICE2021 (**2022**) 035 [arXiv:2203.06777].
[81] C. Jung *et al.*, Columbia Physics System (CPS), https://github.com/RBC-UKQCD/CPS-public.
[82] C. Jung, (RBC and UKQCD Collaborations), Overview of Columbia physics system, Proc. Sci. LATTICE2013 (**2014**) 417.
[83] M. Bruno, pyobs (2023), 10.5281/zenodo.7546851.